

Inhibition of Casein Kinase II by CX-4945, But Not Yes-associated protein (YAP) by Verteporfin, Enhances the Antitumor Efficacy of Temozolomide in Glioblastoma



Xiangyu Liu*, Jieyu Chen[†], Wei Li[†], Chunhua Hang* and Yuyuan Dai[‡]

*Department of Neurosurgery, Drum Tower Hospital, Medical School of Nanjing University, Nanjing, China;

[†]Department of Pathology, Drum Tower Hospital, Medical School of Nanjing University, Nanjing, China; [‡]Model Animal Research Center, Nanjing University, Nanjing, China

Abstract

Overcoming temozolomide (TMZ) resistance in glioma cancer cells remains a major challenge to the effective treatment of the disease. Increasing TMZ efficacy for patients with glioblastoma (GBM) is urgently needed because TMZ treatment is the standard chemotherapy protocol for adult patients with glioblastoma. O⁶-methylguanine-DNA-methyltransferase (MGMT) overexpression is associated with TMZ resistance, and low MGMT is a positive response marker for TMZ therapy. Here, we used 3 glioma cell lines (SF767, U373, and LN229), which had different levels of TMZ sensitivity. We found TMZ sensitivity is positively correlated with MGMT expression and multidrug-resistance protein ABC subfamily G member 2 (ABCG2) in these cells. CK2-STAT3 signaling and Hippo-YAP signaling are reported to regulate MGMT expression and ABCG2 expression, respectively. We combined CK2 inhibitor CX-4945 and YAP inhibitor verteporfin with TMZ treatment. We found that CX-4945 but not verteporfin can sensitize TMZ-resistant cells SF767 to TMZ and that CX-4945 and TMZ combinational treatment was effective for glioma treatment in mouse models compared with TMZ alone. Implications

A combination of CK2 inhibitor with TMZ may improve the therapeutic efficiency of TMZ toward GBM with acquired resistance.

Translational Oncology (2020) 13, 70–78

Introduction

Glioblastoma (GBM) is the most common and malignant primary tumor of the central nervous system, and the prognosis for patients is often poor. The median survival duration of patients with GBM is 15–23 months, and 5-year survival rate is less than 6% [1,2]. The

prognosis for patients with recurrent GBM is even poorer, with an average survival time of around half a year [3].

The treatment of glioblastoma remains difficult, and currently no treatments are curative. Upon initial diagnosis of GBM, present standardized treatment of primary GBM consists of maximal surgical resection, radiotherapy, and concomitant and adjuvant chemotherapy with temozolomide (TMZ). The median survival duration was 14.6 months with radiotherapy plus TMZ and 12.1 months with radiotherapy alone. The two-year survival rate was 26.5% with radiotherapy plus TMZ and 10.4% with radiotherapy alone. The addition of TMZ to radiotherapy for newly diagnosed patients with glioblastomas clearly beneficial [4].

TMZ is an alkylating reagent that can induce DNA methylation of guanine at O⁶ position. The O⁶-methyl-guanine incorrectly pairs with thymine and triggers the mismatch repair system, leading to double strand break of the genome and the following cell cycle arrest and cell apoptosis. O⁶-methylguanine-DNA-methyltransferase

Address all correspondence to: Yuyuan Dai, PhD, Assistant Professor of Nanjing University, 12 Xuefu Road, Nanjing, Jiangsu, 210061, China. E-mail: yuyuandai@gmail.com or Chunhua Hang, MD, PhD, Director at Department of Neurosurgery of Drum Tower Hospital, professor of Medical School of Nanjing University, 321 Zhongshan Road, Nanjing, Jiangsu, 210006, China. E-mail: hang_neurosurgery@163.com
Received 27 May 2019; Revised 17 September 2019; Accepted 19 September 2019

© 2019 The Authors. Published by Elsevier Inc. on behalf of Neoplasia Press, Inc. This is an open access article under the CC BY-NC-ND license (<http://creativecommons.org/licenses/by-nc-nd/4.0/>).
1936-5233/19
<https://doi.org/10.1016/j.tranon.2019.09.006>

(MGMT) can repair the DNA damage caused by TMZ in tumor tissues and prevent tumor cell death. So, a low MGMT level in GBM tissue is regarded as one of positive response markers of TMZ [5,6]. Finding options to suppress MGMT expression can improve the efficacy of TMZ.

Recent evidence suggests casein kinase II (CK2) is a promising therapeutic target for GBM. CK2 is a serine/threonine kinase composed of two catalytic subunits (CK2 α or CK2 α') and two regulatory subunits (CK2 β). *CSNK2A1* gene, encoding CK2 α , has gene amplification in glioblastoma (33.7%). CK2 transcripts and proteins are overexpressed in GBM samples. CK2 inhibition was shown to decrease cell migration and adhesion, increase cellular apoptosis, and inhibit tumor growth in GBM cells [7]. *In vivo*, CK2 inhibitor CX-4945 promotes survival of mice with intracranial human glioblastoma xenografts. However, the relationship between CK2 and TMZ sensitivity has not yet been assessed.

Another way to improve TMZ efficacy is to inhibit the drug efflux ability of adenosine triphosphate-binding cassette (ABC) transporters that played important roles in multidrug resistance (MDR). ABC subfamily B member 1 [ABCB1/P-glycoprotein], ABC subfamily G member 2 [ABCG2, also known as breast cancer-resistance protein], and ABC subfamily C member 1 (ABCC1/MRP1) are the major ABC transporters involved in MDR development [8,9]. The compound efflux ability of ABC transporters also serves as the basis of flow cytometry-based cell-sorting assay called the side population (SP) assay [10]. Cells with high efflux ability reside at the low-left corner in flow cytometry data.

In this study, we used three GBM cell lines to test TMZ sensitivity and study the combinational effect of CK2 inhibitor CX-4945 and TMZ *in vitro* and *in vivo*. The underlying mechanism between CK2 and TMZ sensitivity was elucidated.

Materials and Methods

Cell Culture

LN229 and U373 were established human GBM cell lines (originally purchased from the American Type Culture Collection, Manassas, VA). SF767 was kindly provided by Dr. Fan (University of California, San Francisco, CA). GBM cells were cultivated in DMEM medium supplemented with 10% fetal bovine serum, 100 units/ml penicillin, 100 μ g/ml streptomycin, and 1% L-glutamine (Invitrogen). Culture flasks were kept at 37°C and 5% CO₂ in a humidified atmosphere.

Ethics Statement

Animal experiments were performed following the international guidelines for the care and use of laboratory animals and with Nanjing University Ethical Committee approval.

Animal Study

Six-week-old male RAG-KO mice were maintained and kept in the animal center of Nanjing University. The mice were housed in a temperature-controlled and light-controlled environment. SF767 cells (1×10^5 cells in 100 μ L of DMEM medium) stably transfected with a luciferase expression plasmid (SF767-Luc) were injected into the brains of the mice at 3-mm depth into the brain parenchyma and 3 mm to the right of the midline behind the bregma using a Hamilton syringe under anesthesia with chloral hydrate (4%, 2 mL/kg, *i.p.*). Three days after inoculation, the mice were randomly divided into three groups (nine mice per group). Treatment was initiated after 7 days of tumor cell implantation, according to the following regimens:

(1) control groups receive appropriate vehicles (0.5% dimethyl sulfoxide [DMSO] in PBS); (2) TMZ (100 mg/kg, daily by oral gavage); and (3) TMZ (100 mg/kg, daily by oral gavage) plus CX-4945 (75 mg/kg, twice per day by oral gavage). In the survival study, mice were allowed access to food and water *ad libitum*. Tumor growth was assessed twice a week by bioluminescence imaging using a Xenogen *in vivo* imaging system. We weighed the mice daily, checked survival, and recorded the time until they reached their humane end-points. Humane end-points were defined as the loss of more than 20% of maximum body weight or hunched appearance (in accordance with the ethical committee). Moribund mice were humanely sacrificed by using CO₂, followed by cervical dislocation. At the end of the experiment, the mice were euthanized, and the brains were fixed in 10% buffered formalin, embedded in paraffin, and then stained with Ki67 and cleaved caspase-3. The slides were photographed using a phase-contrast microscope.

Reagents and Antibodies

DMSO was purchased from Sigma (St Louis, MO); TMZ, CX-4945, and verteporfin were purchased from Selleck (Houston, TX) and were dissolved in DMSO for *in vitro* studies. A maximum dose of 0.1% DMSO was never exceeded. The antibodies to pSTAT3 (Tyr705), STAT3, MGMT, YAP, ABCG2, CK2 α , Ki-67, p62, phospho γ -H2AX (Ser139), p53, and GAPDH were obtained from Cell Signaling Technology (Danvers, MA); the Cell Counting Kit-8 (CCK-8) was purchased from Dojindo Molecular Technologies, Inc. (Rockville, MA); the Pierce BCA Protein Assay Kit was obtained from Thermo Scientific Corp (Hudson, NH); the HRP-linked secondary antibodies were from GE Healthcare Bio-Sciences Corp (Piscataway, NJ); and other Western blot reagents were obtained from Bio-Rad Laboratories (Hercules, CA). All cell culture products were purchased from Invitrogen Corp.

Cell Viability Assay

Cell viability was measured by CCK-8 assay. Briefly, SF767, LN229, and U373 cells were plated in 96-well plates (5×10^3 cells/well) and subjected to different treatments. We used DMSO as a vehicle for drug treatment. After 48 h of incubation at 37°C in a humidified atmosphere containing 5% CO₂/95% air, 5 μ L of CCK-8 reagent was added to the cells. The plates were read at 450 nm on a multiscan plate reader after 2 h of incubation.

Western Blot Analysis

Total protein was extracted from cells with M-PER Mammalian Protein Extraction Reagent (Thermo Fisher Scientific, Fremont, CA) supplied with Complete Protease Inhibitor Cocktails (Roche, Lewes, UK), according to manufacturers' protocols. The protein concentrations were measured using the Pierce BCA Protein Assay Kit (Thermo Fisher Scientific, Fremont, CA). Equal amounts of protein diluted in NuPAGE-sample buffer containing reducing reagents were denatured at 95°C for 5 min and electrophoretically separated by 16% sodium dodecyl sulfate-polyacrylamide gel electrophoresis. Proteins were transferred onto nitrocellulose membranes, and the membranes were blocked in 5% BSA in 0.05% Tween-20 and TBS-Standard buffer (25 mM Tris-HCl, 137 mM NaCl, and 2.7 mM KCl) for an hour at room temperature. The blots were probed with the respective primary antibodies followed by their dilution factors [pSTAT3 (Tyr705) 1:1000, STAT3 1:1000, YAP 1:1000, ABCG2 1:1000, MGMT 1:1000, phospho γ -H2AX (Ser139) 1:1000, p53 1:1000 and

GAPDH 1:2000] at 4°C overnight. The membranes were rinsed with PBS and incubated with horseradish secondary antibodies. Protein bands were detected using the ECL detection system (BeyoECL Plus, Beyotime Biotechnology) and quantitatively analyzed using the ImageJ software. The values of each protein were normalized to those of GAPDH. The experiments were performed in triplicate wells and repeated at least three times.

Immunohistochemistry

Solid tumors from sacrificed mice were formalin-fixed and paraffin-embedded. For antigen retrieval, 1 mM ethylenediaminetetraacetic acid (pH 8.0) was used, and methanol containing 3% hydrogen peroxide was used to quench endogenous peroxidase activity. After 2 h of incubation at room temperature with normal goat serum, the slides were incubated at 4°C overnight with primary antibodies (1:50 Ki-67 and 1:50 cleaved-caspase 3). Then, the sections were rinsed with PBS and incubated with horseradish peroxidase-linked goat antirabbit antibodies, followed by reaction with diaminobenzidine. The immunostained sections were counterstained using hematoxylin.

Immunofluorescence

SF767 cells were plated in six-well plates on glass coverslips. After drug treatment for 12 h, cells were washed with PBS (pH 7.2), fixed with 4% paraformaldehyde, and permeabilized with 20 mM Tris HCl (pH 8.0), 50 mM NaCl, 3 mM MgCl₂, 300 mM sucrose, and 0.5% v/v Triton X-100 for 15 min at room temperature. Cells were then rinsed twice with PBS for 5 min each. Cells were blocked with 1% bovine serum albumin in PBS for 1 h and incubated with 1:800 antiphospho γ -H2AX (Ser139) at 4°C overnight. After washing with PBS, phosphor γ -H2AX (Ser139) was detected by incubation for 30 min with antirabbit antibody labeled with Alexa Fluor 555 Conjugate. The nuclear DNA was stained with 1 μ M of Hoechst 33342 for 4 min. Cells were mounted in Shandon Immu-Mount medium.

Tumorsphere Assay

One cell per μ l single-cell suspensions were prepared in StemPro MSC SFM Basal Medium CTS plus StemPro MSC SFM Supplement CTS (Life Technologies), 2 nM L-glutamine, and penicillin (100 IU/ml). Then, 200 μ l (200 cells per well) of the cells were plated in 96-well ultralow attachment plates (Corning Incorporated). For each treatment, seed cells into the wells of two rows for a total of 20 wells. Tumorsphere were cultured for 7 days. Tumorsphere formed in nonadherent cultures were counted under a 10X objective lens. The cutoff size for the spheres counted was 60 μ m.

Side Population Assay

Cells were treated with 0.1% DMSO (control) or 1 μ M verapamil for 72 h, trypsinized and resuspended in DMEM with 2% (v/v) FBS medium at 1×10^6 cells/ml concentration, and incubated with 5 μ g/ml of Hoechst 33343 dye in the presence or absence of 100 μ M verapamil at 37°C for 60 min. Tubes were gently inverted every 20 min and then centrifuged at $400 \times g$ for 5 min at 4°C. The pellets were resuspended in cold PBS containing 2 μ g/ml of propidium iodide and analyzed on a BD FACS Aria II cell sorter. Emission was collected through a 610-nm long pass dichroic mirror to a 620-nm long pass filter for the Hoechst red (x-axis) collection and a 424/44-nm band pass filter for the Hoechst blue (y-axis) collection. The SP was identified as a group of cells able to exclude the Hoechst

dyes, a characteristic inhibited with verapamil. In each experiment, the SP gate was set on the basis of the 100- μ M verapamil control sample. The detailed step-by-step gating strategy to exclude debris and dead cells was followed [10].

Statistical Analysis

Data are presented as mean \pm standard deviation from three independent experiments. The comparisons between control and treated groups were done by using Student's t test. Significance in relation to tumor growth in mice with drug treatment was analyzed using two-way analysis of variance (ANOVA) compared with control mice group. The combination treatment differed from TMZ alone treatment, which was analyzed using two-way ANOVA after Bonferroni post hoc test. Significance in relation to survival was analyzed using the Kaplan-Meier survival curves and the log-rank test. In all experiments, differences were considered statistically significant when $P < 0.05$.

Result

1. MGMT and ABCG2 protein levels are positively correlated with TMZ sensitivity in SF767, U373, and LN229.

To find ways to increase GBM cell lines' sensitivity to TMZ, we first measured the IC₅₀s of TMZ in 3 GBM cell lines SF767, U373, and LN229 (Figure 1A). The IC₅₀s of TMZ decreased in descending order in SF767 ($619.9 \pm 30.5 \mu\text{M}$), U373 ($175.9 \pm 17.3 \mu\text{M}$), and LN229 ($275.1 \pm 78.3 \mu\text{M}$), which means SF767 is the most resistant cell line among these three cell lines. The TMZ efficacy can be regulated by MGMT activity and drug transporter proteins. Thus, we checked the protein level of MGMT by Western blot (Figure 1B). Consistent with the TMZ resistance trend, SF767 has the highest level of MGMT compared with U373 and LN229. Meanwhile, we measured the messenger RNA (mRNA) levels of ABC-transporter ABCG2, ABCB1a, ABCB1b, and ABCC1 by quantitative polymerase chain reaction (Figure 1C) and protein level of ABCG2 by Western blot (Figure 2). SF767 also had the highest mRNA level and protein level of ABCG2.

The SP assay is a widely used technique to measure the drug efflux ability of tumor cells. Our data indicated that consistent with the highest ABCG2 level, SF767 had the highest number of SP population cells (Figure 1D and E), indicating SF767 had the highest drug efflux activity. LN229 had the lowest number of SP population cells. Previous study indicated that SP cells were stem-like cells. To confirm the stem cell properties of these three cell lines, we performed sphere formation assay, which can check the cell self-renewal activity. We found that SF767 and LN229 both can form spheres and had similar sphere numbers while U373 cannot (Figure 1F and G). Even though LN229 had very low SP cell percentage, it still can form spheres. Thus, the non-SP cells may still have self-renewal ability.

2. CK2, pSTAT3, STAT3, and YAP levels are higher in TMZ-resistant cell SF767 than in U373 and LN229.

Previous study indicated that CK2-pSTAT3 signaling can regulate MGMT expression and that Hippo-YAP signaling can regulate ABCG2 expression. We then checked the protein level of CK2, pSTAT3, STAT3, and YAP in SF767, U373, and LN229. We found that SF767 had the highest protein level of CK2, pSTAT3, STAT3, and YAP and that LN229 had the lowest protein level of CK2, pSTAT3, STAT3, and YAP (Figure 2). We wondered if inhibition of

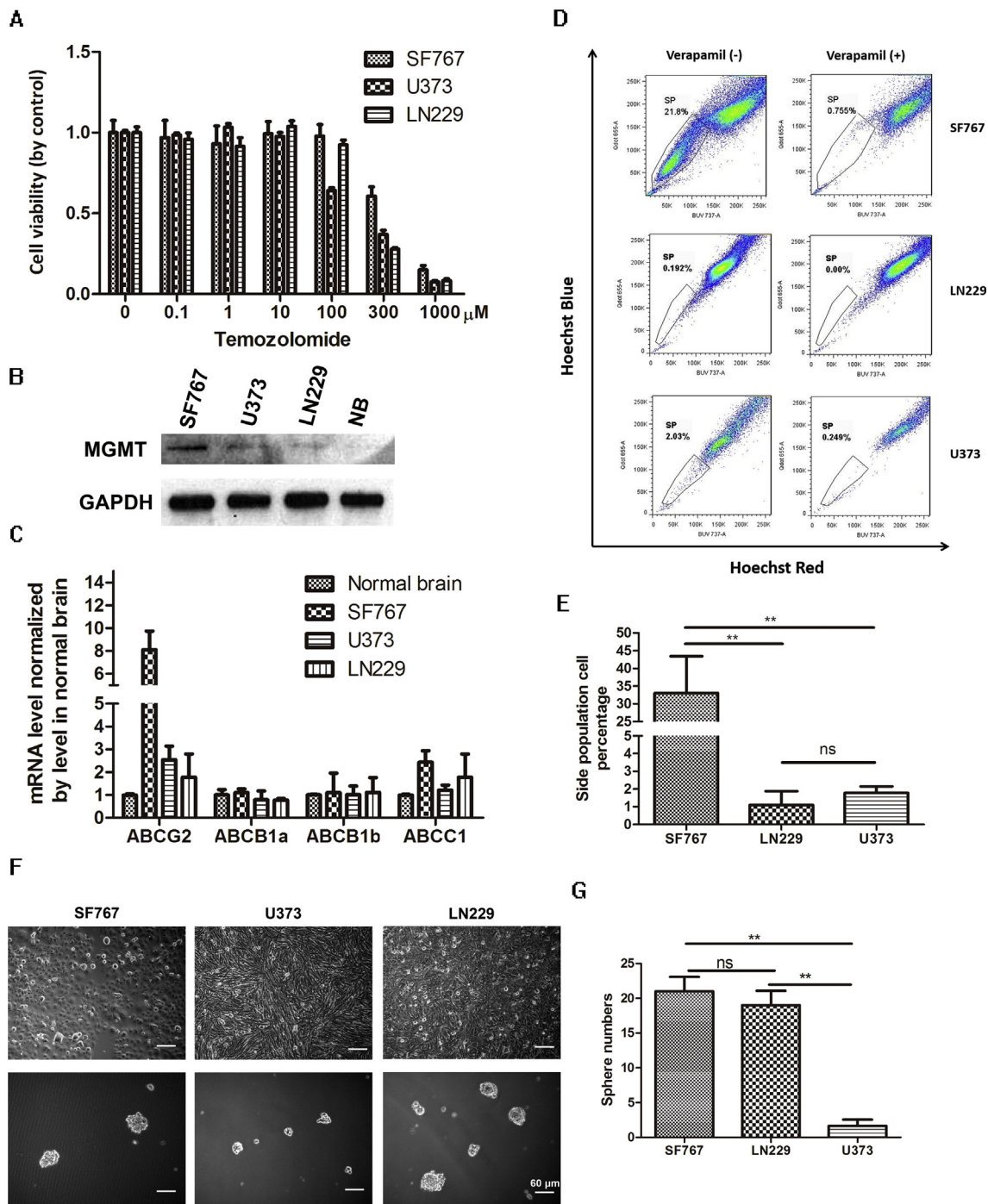


Figure 1. MGMT and ABCG2 protein levels are positively correlated with TMZ sensitivity in SF767, U373, and LN229. (A) Cell viability analysis of SF767, LN229, and U373 cells treated with increasing concentrations of temozolomide. (B) Western blot analysis of MGMT protein level in SF767, U373, LN229, and normal brain tissue. GAPDH was detected as a loading control. (C) qPCR analysis of mRNA level of ABCG2, ABCB1a, ABCB1b, and ABCC1 in glioma cells and normal brain tissues. Data are representative of at least three independent experiments. Error bars indicate the standard deviation of triplicate qPCR data. (D) Flow cytometry analysis of SP cells in SF767, LN229, and U373. (E) Bar graph showing the percentage of SP cells in glioma cells. (F) Image of monolayer cell growth and sphere formation of glioma cells. (G) Bar graph showing the number of spheres formed in glioma cells. Data are representative of at least three independent experiments. * $P < 0.05$, ** $P < 0.005$, *** $P < 0.001$.

CK2 and YAP could decrease MGMT and ABCG2 protein levels, which may increase TMZ sensitivity in glioma cells.

3. Inhibition of CK2 by CX-4945 and inhibition of YAP by verteporfin downregulated MGMT level and ABCG2 level, respectively.

CX-4945 is the specific kinase inhibitor of CK2, and verteporfin is the protein interaction inhibitor of YAP-TEAD complex, which can inhibit YAP cotranscriptional activity. First, we checked the cell viability under different concentrations of CX-4945 or verteporfin. The IC_{50} s of SF767, U373, and LN229 to CX-4945 are 16.72 μM,

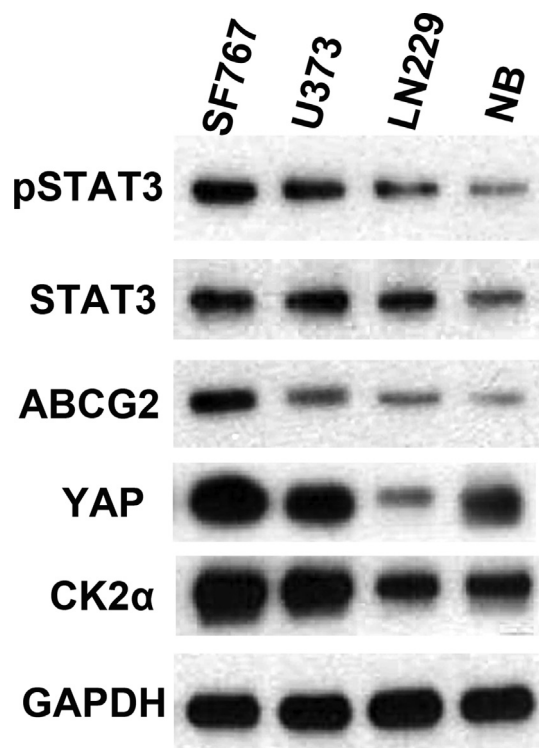


Figure 2. CK2, pSTAT3, STAT3, and YAP levels are higher in TMZ-resistant cell SF767 than in U373 and LN229. Western blot analysis of pSTAT3, STAT3, ABCG2, YAP, and CK2 α protein levels in SF767, U373, LN229, and normal brain tissue. GAPDH was detected as a loading control.

21.19 μ M, and 30.52 μ M, respectively (Figure 3A). The IC₅₀s of SF767, U373, and LN229 to verteporfin are 27.07 μ M, 9.281 μ M, and 5.050 μ M, respectively (Figure 3B). Treatment with 1 μ M CX-4945 or 1 μ M verteporfin to SF767, U373, and LN229 did not cause cell death and was similar to vehicle (DMSO) treatment. CX-4945 of 3 μ M decreased survival LN229 cell percentage to 87.0% but did not affect SF767 and U373. 3 μ M verteporfin decreased survival U373 cell percentage to 86.2% but did not affect SF767 and LN229.

Even though 1–3 μ M of CX-4945 or verteporfin did not cause much measurable glioblastoma cell death, we checked if CK2 was inhibited by CX-4945 and if YAP was inhibited by verteporfin in GBM cells. By Western blot, we found that nondetrimental concentration of CX-4945 treatment decreased the pSTAT3 level, which was a target of CK2 kinase, and MGMT level, which was positively regulated by pSTAT3 (Figure 3C). Nondetrimental concentration of verteporfin treatment decreased YAP protein level and ABCG2 level (Figure 3D). Verteporfin also decreased SP cell percentage in SF767 using SP assay (Figure 3E). These data indicated CX-4945 and verteporfin successfully entered the GBM cells and performed their inhibition activity.

4 Inhibition of CK2 but not inhibition of YAP enhanced TMZ sensitivity in glioma cells.

Overcoming TMZ resistance in glioma cancer cells remains a major challenge to the effective treatment of the disease. CX-4945 and verteporfin were further examined for their effects on the

sensitivity of SF767, U373, and LN229 glioma cells lines. As shown in Figure 4A–C, treatment with CX-4945 (1 μ M) significantly increased TMZ sensitivity in all three cell lines, with remarkably reduced IC₅₀ values for TMZ in all of these cell lines. However, verteporfin at 1 μ M concentration did not change TMZ sensitivity in glioma cells. Increasing verteporfin concentration to 3 μ M did not make differences (Figure 4D–F). Thus, CK2-STAT3-MGMT signaling regulated glioma cells sensitivity to TMZ, but YAP-ABCG2 signaling did not influence TMZ efficacy. The toxicity of TMZ comes from its induction of double-strand DNA breaks that leads to cell cycle arrest and apoptosis. To study if the synergy effect of CX-4945 is due to the increase of DNA damage caused by TMZ, we checked the level of phosphorylated H2AX (γ -H2AX), a phosphorylated variant of histone 2A that associates with DNA double-strand breaks [11], in SF767 after drug treatment. Clearly, TMZ treatment increased the γ -H2AX level in SF767 compared with control cells (Supplemental Fig. 1). Addition of CX-4945 to TMZ further increased γ -H2AX level. However, CX-4945 alone did not increase γ -H2AX. The Western blot results also showed that CX-4945 addition increased γ -H2AX and p53 levels compared with TMZ alone. All these evidences indicated that CX-4945 enhanced TMZ toxicity in glioma cells by increasing DNA damage.

5 Combined treatment of CX-4945 with TMZ exerts a potent antitumor effect in vivo.

To further determine whether CK2 inhibition can augment the effects of TMZ in vivo, we monitored, measured, and compared the tumor growth inhibition and the survival-promoting effects of combined treatment with CX-4945 and TMZ versus either agent alone in SF767 xenografts (Figure 5A–C). Mice treated with vehicle DMSO exhibited rapid increases in bioluminescence. TMZ treatment initially slowed tumor growth, but this effect was disappeared after 24 days. Mice treated with combination therapy showed longer stable bioluminescence through 56 days. Two-way ANOVA indicated that the drug treatment (TMZ or combination therapy) is effective compared with vehicle treatment ($P < 0.05$). Meanwhile, combination therapy is more effective than TMZ treatment alone ($P < 0.05$). From the survival data, we observed that TMZ and CX-4945 together inhibited tumor growth in a prolonged and significant fashion and promoted survival (Figure 5C). The remarkable decrease in tumor cell proliferation (Ki67) and increase in apoptosis (cleaved caspase-3) noted in combination-treated xenografts showed that CK2 inhibition enhance the antitumor activity of sorafenib in glioblastoma (Figure 5D).

Discussion

CK2 α amplification is found in more than 50% of human patients with GBM, and overexpression of CK2 α is associated with worse prognosis. This evidence makes CK2 an intriguing target for preclinical studies in GBM [7]. And CK2 inhibits DNA repair in some context, providing a rational for combining CK2 inhibitors such as CX-4945 with chemotherapy agents that cause DNA damage. Actually, there is an ongoing phase I/II clinical trial on patients with cholangiocarcinoma combining CX-4945 with gemcitabine and cisplatin [12]. Here, we tested the combination effects of CX-4945 with TMZ, and we found that combination of CX-4945 sensitized glioma cells and TMZ treatment in in vitro and in vivo mouse intracranial GBM models, which may be partially through

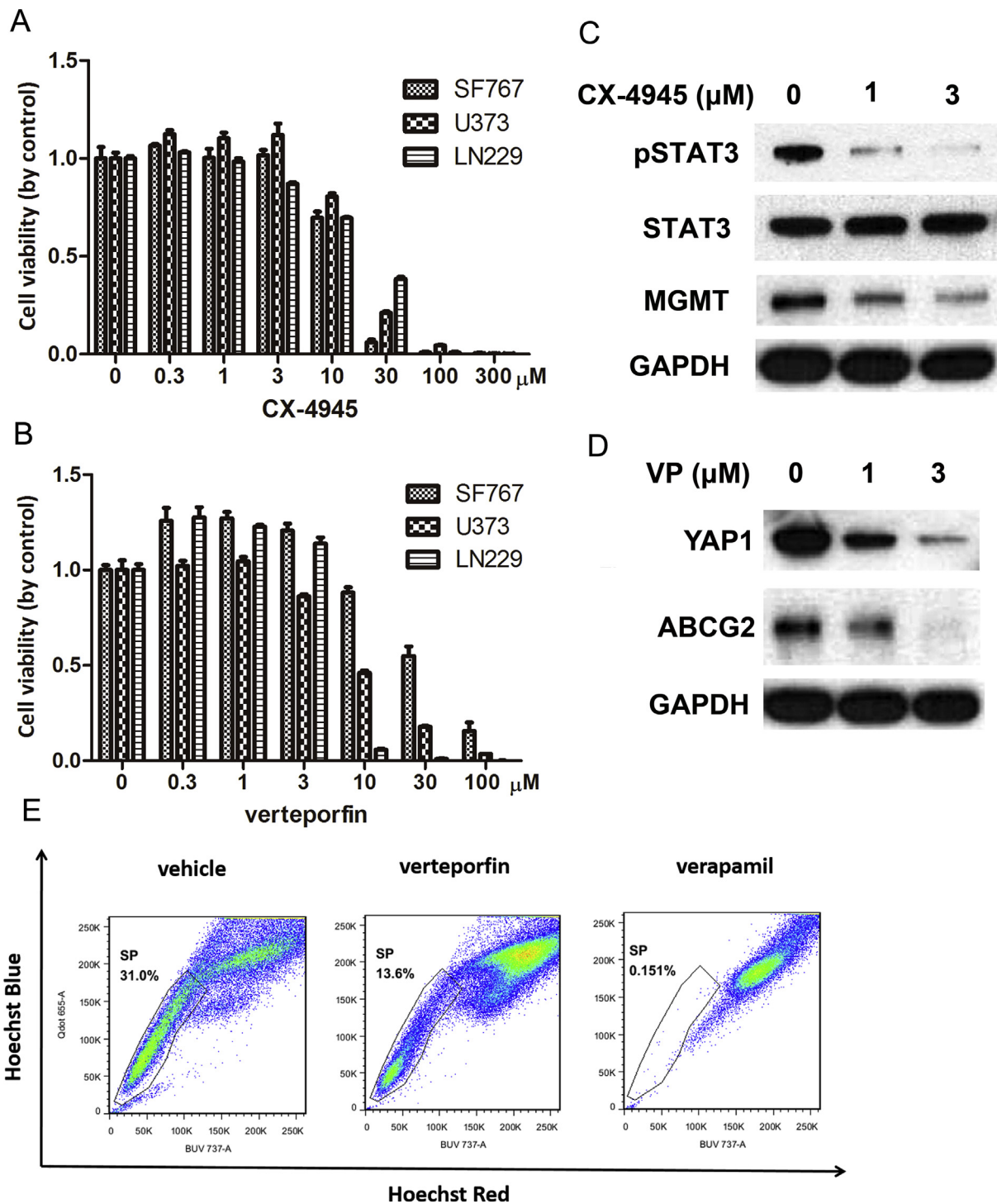


Figure 3. Inhibition of CK2 by CX-4945 and inhibition of YAP by verteporfin downregulated MGMT level and ABCG2 level, respectively. (A–B) Cell viability analysis of SF767, LN229, and U373 cells treated with increasing concentrations of CX-4945 and verteporfin. (C) Western blot analysis of pSTAT3, STAT3, MGMT, and GAPDH protein levels in SF767 after 0-, 1-, and 3-µM CX-4945 treatment. (D) Western blot analysis of YAP1, ABCG2, and GAPDH protein levels in SF767 after 0-, 1-, and 3-µM CX-4945 treatment. (E) Flow cytometry analysis of SP cells in SF767 after vehicle, 1-µM verteporfin, and 100-µM verapamil treatment.

downregulation of MGMT by CK2 inhibition. Our data suggest that the pharmacologic inhibition of CK2 with CX-4945 is a promising strategy for the treatment of GBM with concurrent TMZ.

Radiology plus alkylating chemotherapeutic TMZ is a standard therapeutic regimen for the treatment of newly diagnosed adult patients with GBM [13]. However, TMZ response is highly variable

in patients with GBM, and TMZ resistance is a major obstacle. Intrinsic or acquired TMZ resistance is mediated by multiple molecular events. SF767, the most resistant cell type we used, had the highest protein level of CK2, pSTAT3, and MGMT. MGMT overexpression is proved to be a clinical indicator of TMZ resistance [5,6]. CK2 inhibitor CX-4945 decreased pSTAT3 level without

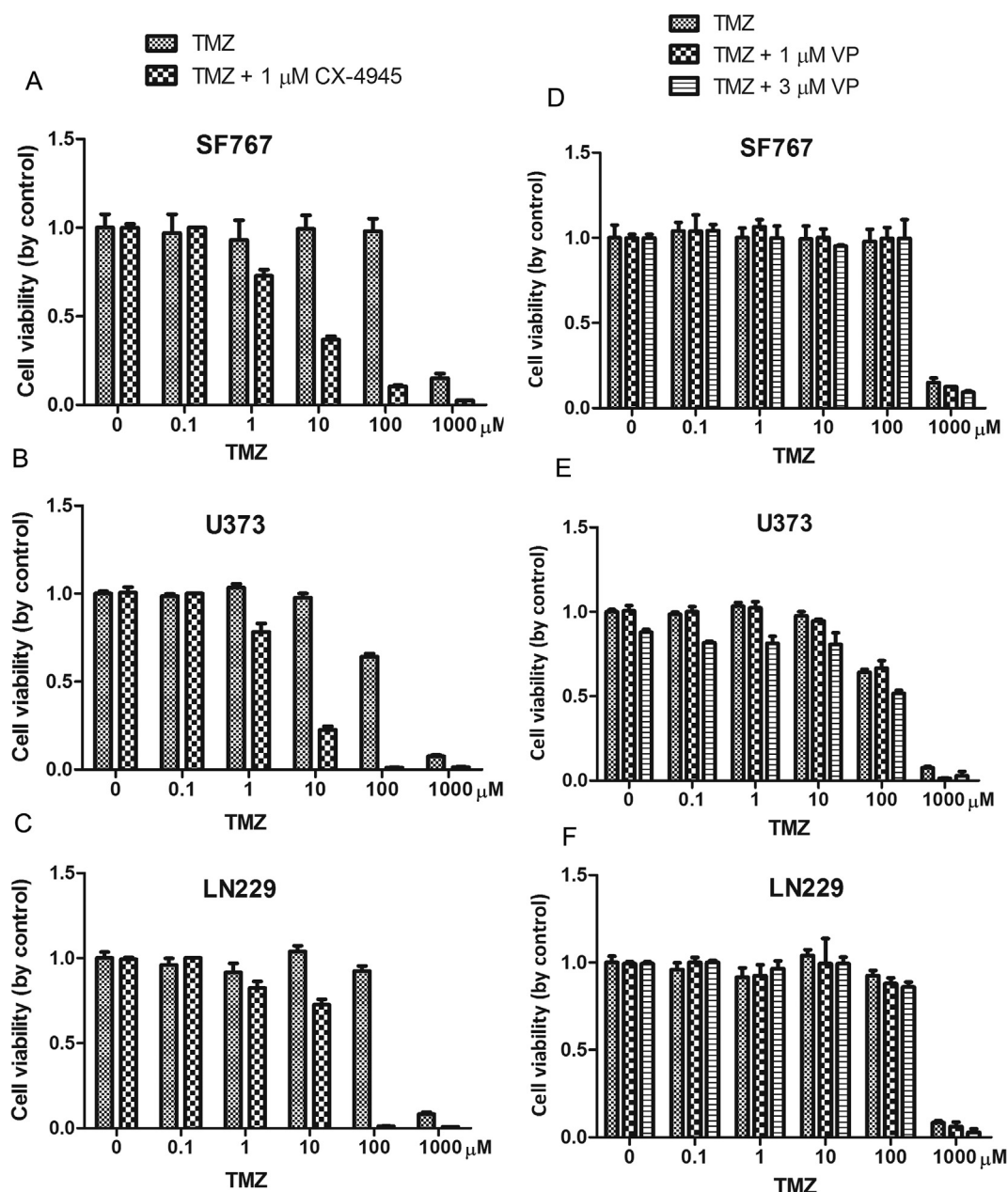


Figure 4. Inhibition of CK2 but not inhibition of YAP enhanced TMZ sensitivity in glioma cells. (A–C) Cell viability analysis of SF767, LN229, and U373 cells treated with increasing concentrations of TMZ and TMZ plus 1- μ M CX-4945. (D–F) Cell viability analysis of SF767, LN229, and U373 cells treated with increasing concentrations of TMZ, TMZ plus 1- μ M verteporfin (VP), and TMZ plus 3- μ M VP.

affecting STAT3 total level and also downregulated MGMT protein expression. More importantly, CX-4945 sensitized TMZ-resistant cell SF767 to TMZ. This evidence indicated CK2-STAT3-MGMT signaling axis might play a role in TMZ resistance. Previous studies indicated CX-4945 inhibits activation of STAT3 and promotes survival of mice with intracranial human glioblastoma xenografts [7,14]. We first reported that CX-4945 can downregulate MGMT expression through inhibition of CK2 in GBM cells.

In intracranial SF767 glioma mouse models, CX-4945 increased TMZ efficacy and prolonged survival of tumor-bearing mouse. However, CX-4945 is only found effective in combination with TMZ when administered on every 6 days rather than regular treatment strategy which is given every/alternate days in intracranial

GL261 (mouse GBM cell line) immunocompetent mouse models [15]. The participation of the immune system of CK2 inhibition was proposed to involve in CX-4945 plus TMZ therapy response. CK2 indeed was found to be a regulator of immunity. CK2 inhibition by CX-4945 could promote Treg cell differentiation and maturation, which may inhibit antitumor immune response [16]. However, in our tumor mouse model, we used immune-deficient mouse. We found an everyday dose of CX-4945 enhanced TMZ efficacy. Further studies using patient-derived xenografts in humanized mouse models to study the effects of CX-4945 with TMZ are needed to clarify the immune suppression effects of CX-4945 for future clinical studies.

An interesting finding is that YAP and ABCG2 are overexpressed in TMZ-resistant GBM cells SF767. The other two ABC transporters,

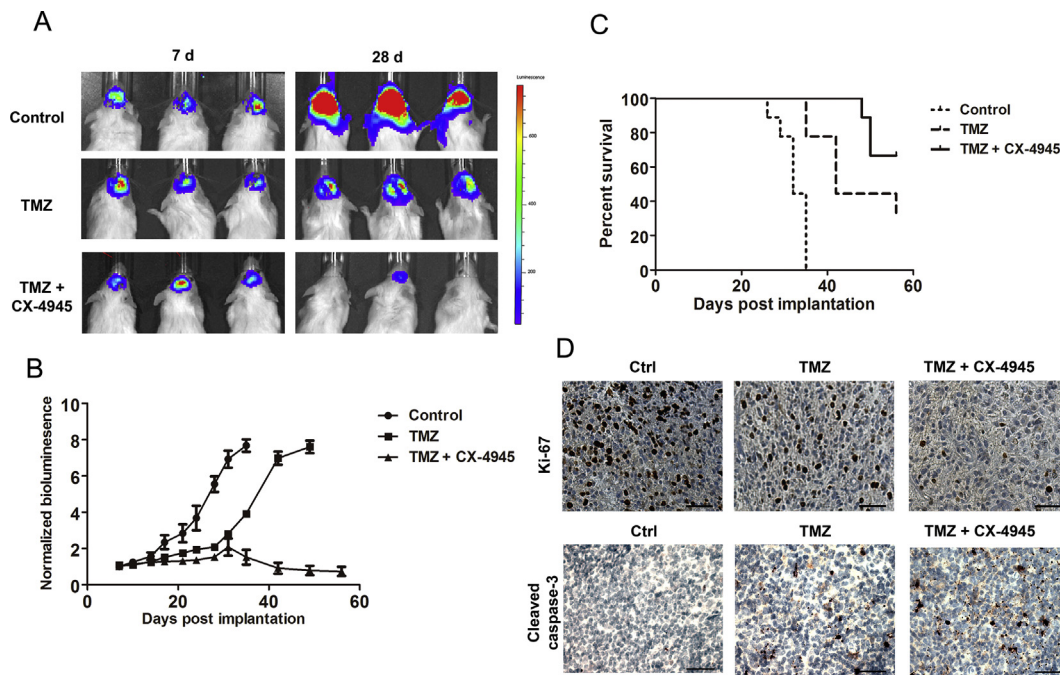


Figure 5. Combined treatment of CX-4945 with TMZ exerts a potent antitumor effect in vivo. (A) Bioluminescence during 28 days of treatment of SF767_Luc tumors ($n = 6$ mice per group). Vehicle, TMZ, TMZ plus CX-4945; (B) Bioluminescence during 56 days of treatment in mice implanted with SF767_Luc cells. The treatment groups differed by two-way ANOVA ($P < 0.05$), and the combination treatment differed from sorafenib-alone treatment after Bonferroni post ($P < 0.05$). (C) Survival curves of SF767_Luc tumor-bearing mice after different treatments. $P = 0.0004$ (Log-rank test) for difference between control and TMZ; $P < 0.0001$ (Log-rank test) for difference between control and TMZ plus CX-4945; $P = 0.0477$ (Log-rank test) for difference between TMZ and TMZ plus CX-4945. (D) Histopathology of sorafenib plus chloroquine shows antiglioma activity, in vivo. Representative brain sections from mice treated with vehicle, TMZ, and TMZ plus CX-4945 were harvested after 28 days, and cell proliferation (Ki67) and apoptosis (cleaved caspase-3) were analyzed. Magnification, $\times 400$.

ABCB1 and ABCC2, were at similar levels in SF767, U373, and LN229. ABCG2 was reported to play a role in TMZ resistance in GBM cells. ABCG2 inhibition by melatonin or Reversan can increase sensitivity to TMZ in in vitro studies [17,18]. We found that SF767 had higher SP cell percentage than U373 and LN229. SP cells were stem-like cells because of their high efflux ability. We used YAP inhibitor verteporfin to inactivate YAP-TEAD transcriptional complex. ABCG2 expression and SP cell percentage were downregulated successfully. However, verteporfin cannot sensitize SF767 to TMZ in vitro. We hypothesized that TMZ was not a substrate of ABCG2. Several other studies also indicated that ABCG2 cannot pump TMZ out of the cells and cannot interfere with TMZ efficacy in the cells [19–22].

Generally, our study found the CK2-pSTAT3-MGMT axis is activated in TMZ-resistant cells SF767. Inhibition of CK2 by CX-4945 can increase TMZ efficacy in vitro and in vivo.

Funding

Yuyuan Dai received Fundamental Research Funds from the Central Universities, China (grant no: 090314380027) and also supports from the National Science Foundation for Young Scholar of China (grant no.: 81802921). Xiangyu Liu received Fundamental Research Funds from the Central Universities, China (grant no: 14380397).

Conflict of interest

The authors declare no potential conflicts of interest.

Appendix A. Supplementary data

Supplementary data to this article can be found online at <https://doi.org/10.1016/j.tranon.2019.09.006>.

References

- [1] Ostrom QT, Gittleman H, Kruchko C, Louis DN, Brat DJ and Gilbert MR, et al (2016). Completeness of required site-specific factors for brain and CNS tumors in the Surveillance, Epidemiology and End Results (SEER) 18 database (2004–2012, varying). *Journal of neuro-oncology* **130**, 31–42.
- [2] Shergalis A, Bankhead 3rd A, Luesakul U, Muangsin N and Neamati N (2018). Current challenges and opportunities in treating glioblastoma. *Pharmacol Rev* **70**, 412–445.
- [3] Wang Y, Kong X, Guo Y, Wang R and Ma W (2017). Continuous dose-intense temozolomide and cisplatin in recurrent glioblastoma patients. *Medicine* **96**, e6261.
- [4] Stupp R, Mason WP, van den Bent MJ, Weller M, Fisher B and Taphoorn MJ, et al (2005). Radiotherapy plus concomitant and adjuvant temozolomide for glioblastoma. *N Engl J Med* **352**, 987–996.
- [5] Hegi ME, Diserens AC, Gorlia T, Hamou MF, de Tribolet N and Weller M, et al (2005). MGMT gene silencing and benefit from temozolomide in glioblastoma. *N Engl J Med* **352**, 997–1003.
- [6] Miyazaki M, Nishihara H, Terasaka S, Kobayashi H, Yamaguchi S and Ito T, et al (2014). Immunohistochemical evaluation of O6-methylguanine DNA methyltransferase (MGMT) expression in 117 cases of glioblastoma. *Neuropathology: official journal of the Japanese Society of Neuropathology* **34**, 268–276.
- [7] Zheng Y, McFarland BC, Drygin D, Yu H, Bellis SL and Kim H, et al (2013). Targeting protein kinase CK2 suppresses prosurvival signaling pathways and growth of glioblastoma. *Clin Cancer Res: an official journal of the American Association for Cancer Research* **19**, 6484–6494.
- [8] Drean A, Rosenberg S, Lejeune FX, Goli L, Nadaradjane AA and Guehennec J, et al (2018). ATP binding cassette (ABC) transporters: expression and clinical value in glioblastoma. *Journal of neuro-oncology* **138**, 479–486.

- [9] Falasca M and Linton KJ (2012). Investigational ABC transporter inhibitors. *Expert Opin Investig Drugs* **21**, 657–666.
- [10] Golebiewska A, Brons NH, Bjerkvig R and Niclou SP (2011). Critical appraisal of the side population assay in stem cell and cancer stem cell research. *Cell stem cell* **8**, 136–147.
- [11] Sharma A, Singh K and Almasan A (2012). Histone H2AX phosphorylation: a marker for DNA damage. *Methods Mol Biol* **920**, 613–626.
- [12] Siddiqui-Jain A, Bliesath J, Macalino D, Omori M, Huser N and Streiner N, et al (2012). CK2 inhibitor CX-4945 suppresses DNA repair response triggered by DNA-targeted anticancer drugs and augments efficacy: mechanistic rationale for drug combination therapy. *Mol Cancer Ther* **11**, 994–1005.
- [13] Mrugala MM and Chamberlain MC (2008). Mechanisms of disease: temozolomide and glioblastoma—look to the future. *Nat Clin Pract Oncol* **5**, 476–486.
- [14] Kohsaka S, Wang L, Yachi K, Mahabir R, Narita T and Itoh T, et al (2012). STAT3 inhibition overcomes temozolomide resistance in glioblastoma by downregulating MGMT expression. *Mol Cancer Ther* **11**, 1289–1299.
- [15] Ferrer-Font L, Villamanan L, Arias-Ramos N, Vilardell J, Plana M and Ruzzene M, et al (2017). Targeting protein kinase CK2: evaluating CX-4945 potential for GL261 glioblastoma therapy in immunocompetent mice. *Pharmaceuticals* **10**.
- [16] Gibson SA, Yang W, Yan Z, Liu Y, Rowse AL and Weinmann AS, et al (2017). Protein kinase CK2 controls the fate between Th17 cell and regulatory T cell differentiation. *J Immunol* **198**, 4244–4254.
- [17] Tivnan A, Zakaria Z, O'Leary C, Kogel D, Pokorny JL and Sarkaria JN, et al (2015). Inhibition of multidrug resistance protein 1 (MRP1) improves chemotherapy drug response in primary and recurrent glioblastoma multiforme. *Front Neurosci* **9**, 218.
- [18] Martin V, Sanchez-Sanchez AM, Herrera F, Gomez-Manzano C, Fueyo J and Alvarez-Vega MA, et al (2013). Melatonin-induced methylation of the ABCG2/BCRP promoter as a novel mechanism to overcome multidrug resistance in brain tumour stem cells. *Br J Canc* **108**, 2005–2012.
- [19] Bleau AM, Hambarzumyan D, Ozawa T, Fomchenko EI, Huse JT and Brennan CW, et al (2009). PTEN/PI3K/Akt pathway regulates the side population phenotype and ABCG2 activity in glioma tumor stem-like cells. *Cell stem cell* **4**, 226–235.
- [20] Oberstadt MC, Bien-Moller S, Weitmann K, Herzog S, Hentschel K and Rimmbach C, et al (2013). Epigenetic modulation of the drug resistance genes MGMT, ABCB1 and ABCG2 in glioblastoma multiforme. *BMC Canc* **13**, 617.
- [21] de Gooijer MC, de Vries NA, Buckle T, Buil LCM, Beijnen JH and Boogerd W, et al (2018). Improved brain penetration and antitumor efficacy of temozolomide by inhibition of ABCB1 and ABCG2. *Neoplasia* **20**, 710–720.
- [22] Natarajan K, Xie Y, Baer MR and Ross DD (2012). Role of breast cancer resistance protein (BCRP/ABCG2) in cancer drug resistance. *Biochem Pharmacol* **83**, 1084–1103.